Available online at www.sciencedirect.com
ScienceDirect
Journal of Catalysis 243 (2006) 165–170
JOURNAL OF CATALYSIS
www.elsevier.com/locate/jcat

Inversion of enantioselectivity for the hydrogenation of ethyl pyruvate in the gas-phase over Pt/SiO_2 modified with derivatives of hydroquinidine

Nicholas F. Dummer [a], Robert Jenkins [a], Xiabao Li [a], Salem M. Bawaked [a], Paul McMorn [a], Andrew Burrows [b], Christopher J. Kiely [b], Richard P.K. Wells [a], David J. Willock [a], Graham J. Hutchings [a,*]

[a] *Department of Chemistry, Cardiff University, P.O. Box 912, Cardiff, CF10 3TB, UK*
[b] *Center for Advanced Materials and Nanotechnology, Lehigh University, Bethlehem, PA 18015-3195, USA*

Received 24 March 2006; revised 10 July 2006; accepted 14 July 2006

Available online 28 August 2006

Abstract

Ethyl pyruvate was hydrogenated as a gas-phase reactant over 2.5% Pt/SiO_2 premodified with hydroquinidine 4-chlorobenzoate at two concentrations (0.85 and 8.5 mM g_{cat}^{-1}). The sense of enantioselectivity changed as a function of the modifier concentration. At low modifier concentrations, the (*S*)-lactate is the preferred product, and at higher concentrations, (*R*)-lactate is favoured. The lower concentration yielded an enantiomeric excess (ee) of 15% (*S*)-ethyl lactate in contrast to 17% (*R*)-lactate for the higher concentration. A range of hydroquinidine and hydroquinine derivatives were evaluated at these concentrations; the results suggest that the carbonyl group of the ester linkage at the C(9) position was required to promote the observed inversion of enantioselectivity. In a subsequent set of experiments, Bi^{3+} was adsorbed onto the Pt/SiO_2 catalyst before the premodification step; these ions are considered to adsorb preferentially on high-energy surface sites (e.g., corner sites or step edges). Increasing Bi^{3+} concentration decreased the degree of inversion until the effect was lost. On the basis of high-resolution electron microscopy (HREM) comparisons of these Pt/SiO_2 and $Bi–Pt/SiO_2$ catalysts, the inversion effect is discussed in terms of the interaction of the substrate and modifier with the catalyst surface.

1. Introduction

Asymmetric hydrogenation of α-ketoesters using supported Pt nanoparticles modified with cinchona alkaloids has been studied extensively and is now considered a model system [1–3]. Recently, Baiker and co-workers [4–7], Bartók and co-workers [8–14], and Murzin and co-workers [15,16] reported a further intriguing aspect of this reaction—that the sense of the enantioselection can be inverted for specific modifiers by changing the extent of reaction [4], the solvent [8], or the substituent at C(9) [5,6]. In all of these cases, the effect is induced by changes in the reaction conditions. Very recently, Bartók and co-workers [14] noted that in the three-phase reactor system (i.e., H_2 gas, liquid reactants and products, and solid catalyst), bulky substituents at the C(9) of the modifier can induce a change in the sense of enantioselection; in particular, the sense of enantioselection is opposite to what was expected. Inversion of enantioselectivity has also been observed by Garland et al. [17] using a continuous-flow three-phase reactor. Note that the observation of changes in the sense of enantioselection is not new; Augustine et al. [18] first observed the effect in 1993 by varying the alkaloid:catalyst concentration using dihydrocinchonidine as modifier with Pt/Al_2O_3 as catalyst for the hydrogenation of ethyl pyruvate; at low modifier concentrations, (*S*)-ethyl lactate formed and at higher modifier levels, the (*R*)-enantiomer formed.

These previous observations of inversion in the sense of enantioselection were all associated with hydrogenation of α-ketoesters in the liquid phase. We wished to investigate

* Corresponding author. Fax: +44 29 20874030.
E-mail address: hutch@cardiff.ac.uk (G.J. Hutchings).

0021-9517/$ – see front matter
doi:10.1016/j.jcat.2006.07.015

whether such effects could be observed using gas-phase reactants, because this would ensure that solvent effects would not complicate this interesting effect.

Gas-phase enantioselective hydrogenation has been rarely reported [19,20], however, such a technique may provide a more simplified approach to determining the mechanism of such reactions. The absence of solvent at and around the reaction interface greatly reduces the complexity of the system. In addition, a greater degree of flexibility with the reaction methodology is afforded, and experiments can be analysed online and reactants switched with minimal disruption to the operating catalyst.

Presented here are the initial investigations into the origin of the intriguing effect of the inversion of enantioselectivity. We have investigated the hydrogenation of ethyl pyruvate (I, Scheme 1) with a commercially prepared Pt/SiO_2 catalyst modified using hydroquinidine modifiers (Scheme 2) leading to the formation of *R*- or *S*-ethyl lactate (II, Scheme 1). We demonstrate that inversion of enantioselectivity can be observed in the absence of solvent when the reaction is carried out at the gas–solid interface, confirming the effect is due to the interaction among the modifier, the substrate, and the metal surface. Furthermore, by careful modification of the alkaloid, the carbonyl of an ester linkage to the carbon at C(9) is significant with regard to this effect.

2. Experimental

2.1. Reactions at the gas–solid interface

Enantioselective hydrogenations were performed over a 2.5% Pt/Silica (Johnson Matthey M01271) catalyst, premodi-

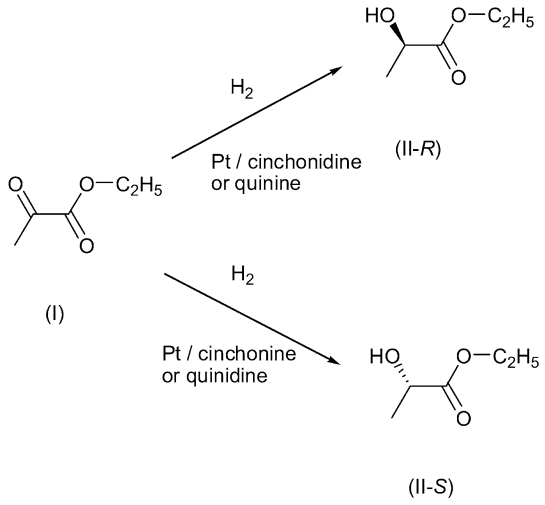

Scheme 1. The possible products of ethyl pyruvate (I) hydrogenation over cinchona modified platinum catalysts.

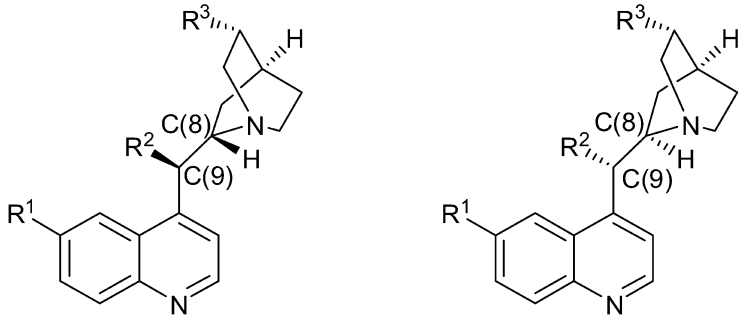

Modifier		Derivative	R^1	R^2	R^3
cinchonine	Cn	2	H	OH	C_2H_3
Cinchonine acetate	CnA	2	H	CH_3COO	C_2H_5
cinchonine phenyl acetate	CnPA	2	H	C_6H_5COO	C_2H_3
hydroquinine 4-chlorobenzoate	HQnClB	2	OMe	p-ClC_6H_4COO	C_2H_5
hydroquinidine	HQd	1	OMe	OH	C_2H_5
hydroquinidine phenyl acetate	HQdPA	1	OMe	C_6H_5COO	C_2H_5
hydroquinidine 4-chlorobenzoate	HQdClB	1	OMe	p-ClC_6H_4COO	C_2H_5
hydroquinidine phenanthryl ether	HQdPAE	1	OMe	C_9H_6NO	C_2H_5
hydroquinidine 4-methyl-2-quinolyl ether	HQdMQE	1	OMe	$C_{14}H_9O$	C_2H_5

Scheme 2. Structures of cinchonidine **1** and cinchonine **2** derivatives.

fied with an appropriate alkaloid. Commercial cinchona alkaloids used included cinchonine (Cn; Fluka, 98%), hydroquinidine (HQd; Aldrich, 95%), hydroquinidine 4-chlorobenzoate (HQdClB; Aldrich, 98%), hydroquinine 4-chlorobenzoate (HQnClB; Aldrich, 98%), hydroquinidine 9-phenanthryl ether (HQdPAE; Aldrich, 96%), and hydroquinidine 4-methyl-2-quinolyl ether (HQdMQE; Aldrich, 97%). Premodification of catalyst samples was conducted on a small batch scale, giving sufficient catalyst for several experiments. Catalyst samples (200 mg) were stirred in a slurry of alkaloid and dissolved in dichloromethane (25 ml) in air for 10 min. Control experiments using nitrogen in place of air showed no differences in catalytic efficacy. The catalyst was filtered and dried under vacuum before being transferred to the glass reactor tube for reaction at 10 °C. Catalyst samples (25 mg) were preconditioned in a He flow (80 ml min^{-1}) for 10 min, followed by a 3:1 He:H_2 flow (80 ml min^{-1}) for a further 10 min. This mixture was then diverted through a saturator (3 °C) containing the reactant. The effluent reaction gas was analysed by on-line gas chromatography at regular intervals during the reaction period. (See [20] for full details and demonstration that the conditions used do not involve gas/liquid/solid systems due to capillary condensation.)

2.2. Addition of Bi^{3+} to the platinum surface

A 1-g sample of 2.5% Pt/SiO_2 was placed in a round-bottomed flask to which aqueous $Bi(NO_3)_3$ (5 ml, 0.15–0.75 mM; Aldrich, 99.999%) dissolved in ultra-pure water was added. The slurry was stirred for 3 h and filtered under vacuum and washed with ultra-pure water (500 ml) to remove any remaining nitrate species. The catalyst was dried under vacuum and used immediately in the alkaloid premodification procedure.

2.3. Synthesis of cinchonine and hydroquinidine derivatives

All reactions were carried out under a dried N_2 atmosphere. All starting materials but cinchonine (98%, Fluka) were purchased from Aldrich and used as received. APCI mass spectra were recorded on a Fisons Platform II spectrometer at a cone voltage of 20 V. ^{1}H NMR spectra were recorded in $CDCl_3$ using a 500-MHz Bruker Avance spectrometer.

2.3.1. Hydroquinidine phenyl acetate (HQdPA)

Hydroquinidine (200 mg, 0.61 mmol) and triethylamine (92.8 mg, 91.7 mmol) were dissolved in dichloromethane (20 ml). The solution was cooled to 0–5 °C, and benzoyl chloride (85.6 mg, 0.61 mmol) was added dropwise. The reaction mixture was allowed to warm to room temperature and stirred at this temperature overnight. The reaction mixture was poured to ice water (50 ml) and extracted with dichloromethane (3 × 30 ml), the combined organic layers were washed with saturated aqueous $NaHCO_3$, dried over Na_2SO_4, and evaporated to dryness. The product was recrystallised from a solution of 10% diethyl ether/light petroleum 40–60.

δ_H (500 MHz, $CDCl_3$) = 8.70 (1 H d), 8.08 (2 H dd), 7.99 (1 H d), 7.58 (1 H t), 7.51 (1 H d), 7.45 (2 H dd), 7.40 (1 H d), 7.35 (1 H dd), 6.81 (1 H d), 3.95 (3 H s), 3.36 (1 H aq), range 2.95–2.65 (4 H m), 1.96 (1 H tt), 1.76 (1 H s), range 1.59–1.47 (6 H m), 0.88 (3 H t). m/z 431 ($M + H^+$).

2.3.2. Cinchonine acetate (CnA)

Cinchonine (100 mg, 0.34 mmol) and triethylamine (51.4 mg, 0.51 mmol) were dissolved in dichloromethane (20 ml). The solution was cooled to 0–5 °C, and acetyl chloride (26.6 mg, 0.34 mmol) was added dropwise. The product was recovered and recrystallised as described previously.

δ_H (500 MHz, $CDCl_3$) = 8.80 (1 H d), 8.13 (1 H d), 8.05 (1 H d), 7.64 (1 H dd), 7.52 (1 H dd), 7.31 (1 H d), 6.50 (1 H d), 5.95 (1 H m), range 5.20–5.00 (2 H m), 3.22 (1 H qa), range 2.85–2.59 (4 H m), 2.19 (1 H qa), 2.05 (3 H s), range 1.80–1.73 (2 H m), range 1.48–1.41 (3 H m). m/z 337 ($M + H^+$).

2.3.3. Cinchonine phenyl acetate (CnPA)

Cinchonine (100 mg, 0.34 mmol) and triethylamine (51.4 mg, 0.51 mmol) were dissolved in dichloromethane (20 ml). The solution was cooled to 0–5 °C, and benzoyl chloride (47.6 mg, 0.34 mmol) was added dropwise. The product was recovered and recrystallised as described previously.

δ_H (500 MHz, $CDCl_3$) = 8.76 (1 H d), 8.28 (1 H d), range 8.07–8.00 (4 H m), range 7.64–7.35 (5 H m), 6.81 (1 H d), 5.93 (1 H ddd), 5.04 (1 H d), 5.00 (1 H d), 3.37 (1 H aq), range 2.99–2.63 (4 H m), 2.23 (1 H aq), 1.94 (1 H t), 1.79 (1 H s), range 1.57–1.47 (3 H m). m/z 399 ($M + H^+$).

2.4. Transmission electron microscopy

Bright-field (BF) and high-resolution transmission electron microscopy (HRTEM) was performed at 200 kV using a JEOL 2200FS transmission electron microscope with a point-to-point resolution of 0.19 nm. Samples were prepared for TEM analysis by dispersing the catalyst powder in high-purity ethanol, then allowing a drop of the suspension to evaporate on a holey carbon film supported by a 300-mesh copper TEM grid.

3. Results and discussion

Recently, we showed that the enantioselective hydrogenation of pyruvate esters can be carried out in the absence of solvent at the gas–solid interface [20]. The significance of this observation is that enantioselective experiments can be conducted in the absence of solvent effects, which are known to be a potentially dominant feature [21]. In view of this, we carried out an extensive set of experiments using gas-phase reactants and investigated the use of various cinchonine and cinchonidine-derived modifiers for the hydrogenation of ethyl pyruvate at the gas–solid interface over a 2.5% Pt/SiO_2 catalyst using two different concentrations of the modifiers. The results are given in Table 1. Under these conditions, 100% conversion was achieved irrespective of the choice of modifier or the presence of alkaloid; this was stable throughout the reaction. Time-on-line data for the two concentrations are given in Fig. 1 for the enantioselectivity of Cn (squares), HQnClB (diamonds), HQdClB (circles), HQdPAE (triangles), and no modifier (crosses). It is

Table 1
The influence of modifier structure and concentration of hydroquinine (**1**) hydroquinidine (**2**) derivatives on the sense of enantioselectivity in the gas phase hydrogenation of ethyl pyruvate

Entry	Modifier	Enantiomeric excess (%)	
		0.85 mM g_{cat}^{-1} [a]	8.50 mM g_{cat}^{-1} [a]
1	Cn	30 (*S*)	27 (*S*)
2	CnA	5 (*S*)	5 (*R*)
3	CnPA	5 (*S*)	5 (*R*)
4	HQnClB	15 (*R*)	10 (*S*)
5	HQd	25 (*S*)	15 (*S*)
6	HQdPA	6 (*S*)	15 (*R*)
7	HQdClB	15 (*S*)	17 (*R*)
8	HQnPAE	8 (*R*)	9 (*R*)
9	HQnMQE	6 (*R*)	16 (*R*)

[a] Modifier concentration.

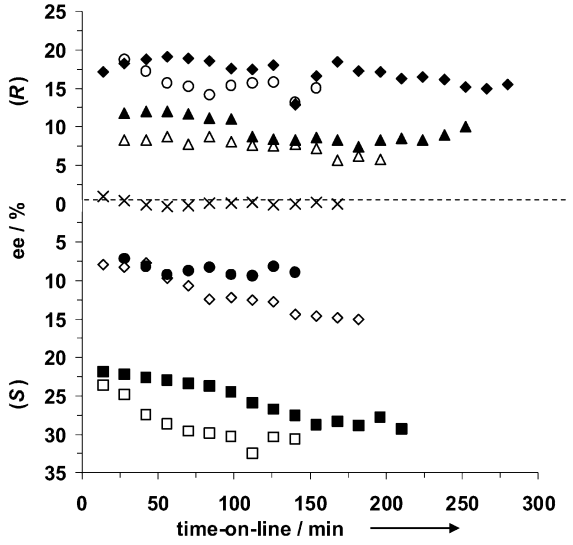

Fig. 1. Time-on-line data of the enantioselective hydrogenation of ethyl pyruvate in the gas phase over 2.5% Pt/SiO_2 (unmodified, crosses) and using a range of chiral modifiers; closed symbols—8.5 mM g_{cat}^{-1}, open symbols—0.85 mM g_{cat}^{-1}. Cn (squares), HQnClB (diamonds), HQdPAE (triangles) and HQdClB (circles). Conditions; 25 mg premodified catalyst, 25% H_2/He, 1 bar pressure, 9600 h^{-1} GHSV, 3 °C saturator, 10 °C reactor.

apparent that inversion of enantioselectivity is observed with HQnClB (Table 1, entry 5) and HQdClB (entry 6). Additionally, this phenomenon was observed with CnPA (entry 2), CnA (entry 3), and HQdPA (entry 7). The effect is considered experimentally significant and has been observed in many repeat experiments.

Consequently, we conclude on the basis of these experiments that the solvent plays no significant effect in the origin of the inversion of enantioselectivity. Furthermore, no initial transient effects are observed (Fig. 1) with modifiers for which inversion of enantioselectivity is observed. However, an initial transient effect is still observed with cinchonine as modifier under the gas-phase conditions, and the effect is most marked when a low concentration of the modifier is used (Fig. 2). These results suggest that the origin of the inversion and initial transient effects are not linked, and neither effect is dependent on solvent involvement.

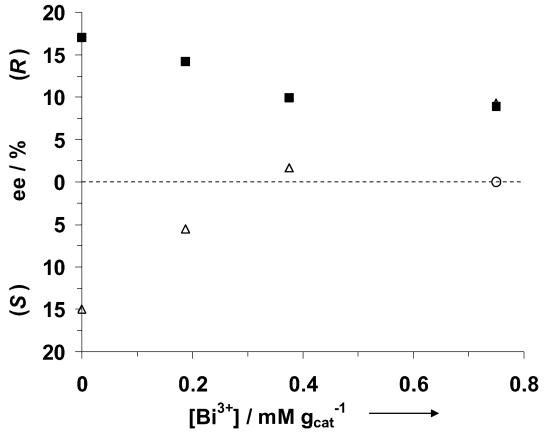

Fig. 2. The influence of increasing the concentration of Bi^{3+} ions on the enantioselective hydrogenation of ethyl pyruvate in the gas phase over 2.5% Pt/SiO_2 with no modifier (○) and using HQdClB: (■) 8.5 mM g_{cat}^{-1}, (△) 0.85 mM g_{cat}^{-1}. Conditions: 25 mg premodified catalyst, 25% H_2/He, 1 bar pressure, 9600 h^{-1} GHSV, 3 °C saturator, 10 °C reactor temperature.

We have found that the observation of inversion of enantioselectivity is dependent on the nature of the substituent at C(9). Inversion is not observed if the substituent at this position is OH (Table 1, entries 1 and 5) or with an ether linkage (Table 1, entries 8 and 9). However, inversion of enantioselectivity is always observed when the C(9) substituent comprises an ester linkage. The steric bulk of the substituent at C(9) does not appear to be a significant factor (Table 1, entries 8 and 9), nor the omission of the OMe group from the quinoline ring (Table 1, entries 2 and 3). We consider the interaction of the substrate with the carbonyl group of the modifier to be the key factor in determining whether inversion of enantioselectivity is observed. Because no initial transient is observed with modifiers that display inversion of enantioselectivity using gas-phase reactants, we consider that the carbonyl group of the substituent interacts strongly with the surface of the Pt nanocrystals, significantly affecting the conformation of the modifier on the surface leading to the origin of this effect.

We wished to determine whether an inversion of enantioselectivity is a function of the nature or morphology of the Pt crystallites as well as the modifier concentration. Recently, Attard et al. [22] reported that addition of Bi^{3+} to platinum single crystals and Pt/C catalysts preferentially adsorb at high-energy surface sites (e.g., step edges, corner sites, kinks in step edges). This effect was exploited to reduce the production of higher-molecular-weight products during pyruvate hydrogenation.

Consequently, we set out to deliberately block these sites in a similar manner, and investigated the effect of adding Bi^{3+} to Pt/SiO_2 before modification with hydroquinidine 4-chlorobenzoate. The results for the enantioselective hydrogenation of ethyl pyruvate at the gas–solid interface as a function of Bi^{3+} concentration are shown in Fig. 3.

Where no alkaloid modification occurs, the resulting lactate product is racemic (Fig. 2, open circles). At low modifier concentrations (open triangles), increasing the concentration of Bi^{3+} sequentially removes the active sites responsible for the *S*-enantiomer formation, until at higher Bi^{3+} concentrations,

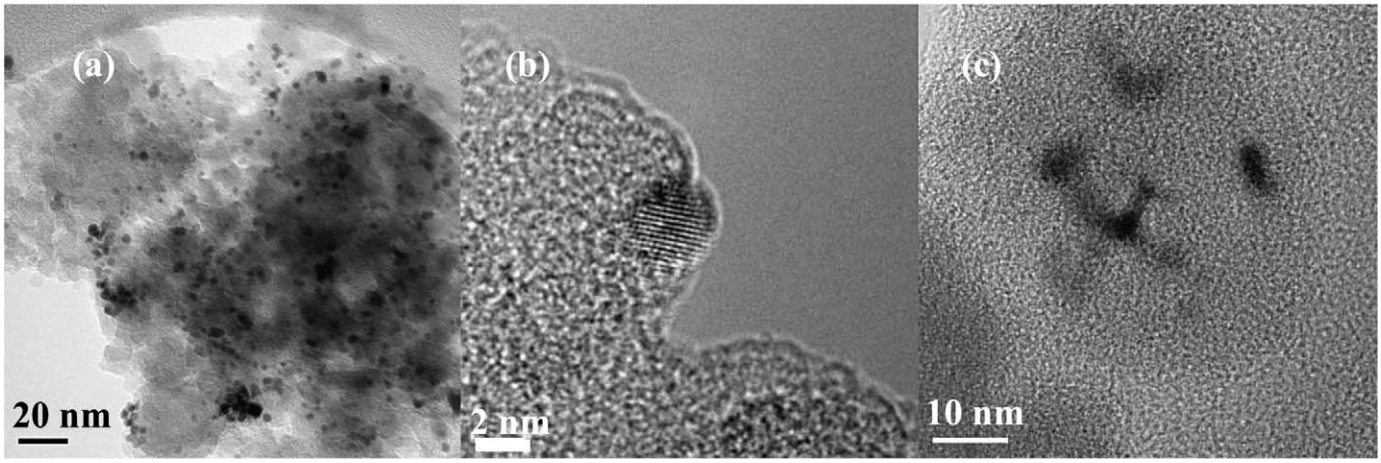

Fig. 3. Bright field transmission electron micrographs of the Pt/SiO_2 (a, b) and $Bi–Pt/SiO_2$ (c) samples showing Pt nanoparticles with a 2–5 nm size distribution and occasional regions where the supported particles apparently wet and spread out on the SiO_2 support material.

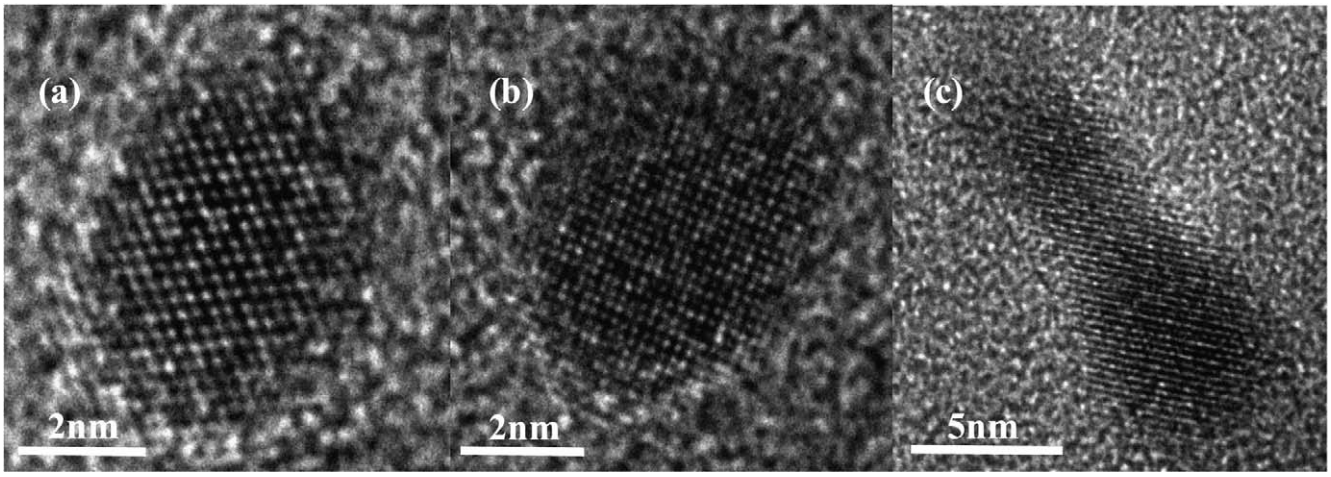

Fig. 4. Representative high resolution electron micrographs of the supported crystallites in the $Pt–Bi/SiO_2$ sample. The nanoparticle orientations as determined from measurements of lattice fringe spacings and inter-planar angles are (a) [110] Pt, (b) [001] Pt and (c) PtO [221].

the *R*-enantiomer is formed in excess. At the higher modifier concentrations (solid squares), which gives the *R*-enantiomer in excess in the absence of Bi^{3+}, a decrease of ca. 6% ee with increasing Bi^{3+} concentration is observed.

TEM was carried out on both the Pt/SiO_2 and $Bi–Pt/SiO_2$ samples to compare their respective microstructures. Fig. 3a is a BF micrograph showing the general morphology of the Pt/SiO_2 material. A dispersion of Pt nanoparticles in the 2- to 5-nm size range is clearly visible by diffraction contrast against the amorphous SiO_2 support in this image. The particle size distribution measured for the corresponding Pt/SiO_2 sample is comparable, which is not unexpected because the heat treatments received by both materials were identical. In both samples, however, two distinct particle morphologies were observed to coexist. The first, and most commonly found morphology by far, comprised truncated cuboctahedral particles of metallic Pt (Fig. 3b). Typical lattice images of such particles viewed along the {110} and {001} directions are shown in Figs. 4a and 4b, respectively. Surface faceting of the cub-octahedral particles to preferentially expose low-energy {111}- and {200}-type planes is apparent. The second, and considerably rarer, morphology shown in Fig. 3c is of particles that appear to "wet" the SiO_2 substrate. These have a considerably weaker contrast level than the purely metallic Pt nanoparticles, suggesting that they are thinner and/or have a lower average atomic mass or density. Measurement of lattice fringe spacings and intersection angles of the particles shown in Fig. 4c are consistent with the {221} projection of PtO. The relative proportions of the Pt to PtO particles appeared to be very similar in the Pt/SiO_2 and $Bi–Pt/SiO_2$ samples, and hence we do not consider the presence of PtO to be an important factor in these studies. Although the presence of Bi in the latter sample was verified by atomic absorption spectroscopy (AAS), X-ray energy dispersive analysis (XEDS) in the TEM was unable to detect this due to the very low concentration of Bi^{3+} present. Furthermore, the low atomic number difference between Pt (78) and Bi (83) atoms meant that discriminating between the two elements by mass contrast in high-angle annular dark field (HAADF) imaging experiments was not possible.

Even though we were unable to detect the presence of Bi in the TEM or to identify and gross changes in microstructure between the Pt/SiO_2 and $Pt–Bi/SiO_2$ samples, it is still worthwhile to speculate on reasons that could explain the origin of

this interesting inversion effect. A possible model is that the chiral modifier forms chiral active sites by adsorption on high-energy kink or edge surface sites of the Pt (i.e., step edges, corner sites, kinks in step edges), and these confer the opposite enantioselective direction to sites formed by adsorption on terrace sites. In this way, the effect is considered analogous to the promotion of supported Pt catalysts for oxidation reactions observed when doped with low concentrations of Bi^{3+}. With Bi-promoted metal catalysts, the effect is considered to be due to Bi^{3+} cations progressively adsorbing on and thereby blocking/poisoning specific surface sites [23] that catalyse nonselective oxidation. Recently, Attard et al. [22] confirmed this result using cyclic voltammetry to probe the interaction between Bi^{3+} and Pt surfaces of both catalyst and single crystals. Hence, at low modifier concentrations, the modifier absorbs at these high-energy surface sites, giving one sense of enantioselectivity, and these sites are present only in low amounts. At higher modifier concentrations, other lower energy surface sites are modified, which give rise to the other sense of enantioselectivity. Hence, the two sites act in opposition and limit the overall enantioselection that can be achieved.

4. Conclusion

In conclusion, we have shown that the sense of enantioselectivity for the hydrogenation of ethyl pyruvate can be a function solely of the modifier concentration over a range of cinchonidine and quinine derivatives **1** and cinchonine and quinidine derivatives **2**. Furthermore, we have shown the effect is independent of solvent, as observed in experiments involving the gas–liquid interface. Our findings have important implications, predicting that 100% enantioselection may not be achieved with this experimental approach, because the modifier interactions with different sites on the heterogeneous catalyst lead to different senses of enantioselection. We note, however, that the effect is very specific to the substitute at the C(9) position, and so the results may be very specific to the systems investigated to date. Our results should now prompt the design of catalyst surfaces with specific surface sites or at least minimising sites that can lead to inversion of enantioselectivity.

Acknowledgments

This work was supported by the Leverhulme Trust (N.F.D.) and King Abdul Aziz University (S.M.B.).

References

[1] M. von Arx, T. Mallat, A. Baiker, Top. Catal. 19 (2002) 75–87.
[2] H.U. Blaser, Chem. Commun. (2003) 293–296.
[3] G. Vayner, K.N. Houk, Y.-K. Sun, J. Am. Chem. Soc. 126 (2004) 199–203.
[4] M. von Arx, T. Mallat, A. Baiker, Angew. Chem. Int. Ed. 40 (2001) 2302–2305.
[5] R. Hess, A. Vargas, T. Mallat, T. Bűrgi, A. Baiker, J. Catal. 222 (2004) 117–128.
[6] S. Diezi, A. Szabo, T. Mallat, A. Baiker, Tetrahedron Asymmetry 14 (2003) 2573–2577.
[7] N. Bonalumi, A. Vargas, D. Ferri, T. Bűrgi, T. Mallat, A. Baiker, J. Am. Chem. Soc. 127 (2005) 8467–8477.
[8] M. Bartók, M. Sutyinski, K. Felföldi, G. Szöllósi, Chem. Commun. (2002) 1130–1131.
[9] G. Szöllósi, G. Somlai, P.T. Szabó, J. Mol. Catal. A 170 (2001) 165.
[10] K. Ferfóldi, T. Varga, P. Forgó, M. Bartók, Catal. Lett. 97 (2004) 65–70.
[11] M. Bartók, M. Sutyinski, I. Busci, K. Ferfóldi, G. Szöllósi, F. Bartha, T. Bartók, J. Catal. 231 (2005) 33–40.
[12] M. Bartók, K. Balázsik, I. Bucsi, G. Szöllósi, J. Catal. 239 (2006) 74–82.
[13] K. Szöri, K. Balázsik, K. Felföldi, M. Bartók, J. Catal. 241 (2006) 149–154.
[14] S. Cserényi, K. Felföldi, K. Balázsik, G. Szöllősi, I. Busci, M. Bartók, J. Mol. Catal. A 247 (2006) 108–115.
[15] E. Toukoniitty, I. Busygin, R. Leino, D.Y. Murzin, J. Catal. 227 (2004) 210–216.
[16] I. Busygin, E. Toukoniitty, R. Leino, D.Y. Murzin, J. Mol. Catal. A 236 (2005) 227–238.
[17] F. Gao, L. Chen, M. Garland, J. Catal. 238 (2006) 402–411.
[18] R.L. Augustine, S.K. Tanielyan, L.K. Doyle, Tetrahedron Asymmetry (1993) 1803–1827.
[19] A. López-Martínez, M.A. Keane, J. Mol. Catal. A Chem. 153 (2000) 257–266.
[20] M. von Arx, N. Dummer, D.J. Willock, S.H. Taylor, R.P.K. Wells, P.B. Wells, G.J. Hutchings, Chem. Commun. (2003) 1926–1927.
[21] T. Bürgi, A. Baiker, J. Am. Chem. Soc. 120 (1998) 12920–12926.
[22] D.J. Jenkins, A.M.S. Alabdulrahman, G.A. Attard, K.G. Griffin, P. Johnston, P.B. Wells, J. Catal. 234 (2005) 230–239.
[23] A.-B. Crozon, M. Bresson, P. Gallezot, New J. Chem. 22 (3) (1998) 269–273.